

Gaussian component of beams with fractional topological charge

Maria Isabella M. Mendoza ^{*}, Nathaniel Hermosa , and Niña Zambale Simon

National Institute of Physics, University of the Philippines Diliman, Philippines

^{*}Corresponding author: mmmendoza31@up.edu.ph

Abstract

Fractional vortex beams, which possess fractional topological charge ℓ , are interesting for allowing finer control of orbital angular momentum (OAM). In this paper, we characterize these kinds of beams by projecting them onto a Gaussian mode. We generated beams with fractional ℓ using an SLM and passed them into a single mode fiber, recording the magnitude of the exiting beam as voltage. We observe that this voltage is maximum for a Gaussian beam ($\ell = 0$) and lowest at or near integer ℓ as predicted. Moreover, we observe that the Gaussian component still manifests at fractional ℓ ; we believe this is due to the absence of vortices on the z-axis as described by Berry [J. Opt. A: Pure Appl. Opt. 6, 259 (2004)]. Our results have provided an alternative method to describe fractional vortex beams, as well as empirical validation for Berry's theoretical work on the fractional vortex beam.

Keywords: vortex beams, fractional topological charge, single-mode fiber, mode projection

1 Introduction

Vortex beams are an example of beams carrying orbital angular momentum (OAM), which manifests as a central region of zero intensity — a vortex. As such, they have been leveraged in fields like particle manipulation, information encoding, and imaging [1]. Their OAM results in a helical wavefront according to their equation of field, given in cylindrical coordinates by: [2]

$$\psi(R, \phi, z) \propto \exp\left(-\frac{R^2}{w_o^2}\right) \exp(i\ell\phi) \quad (1)$$

where R is the position — and ϕ the azimuthal angle — on a plane perpendicular to z , the propagation axis; w_o is the beam waist. The OAM is directly proportional to the “twists” of this wavefront given by the topological charge ℓ [3, 4].

The modes of vortex beams ψ_ℓ are differentiated by the values of ℓ . As the eigenmodes, integer modes are the most readily used for the applications of OAM mentioned above. However, the interest in fractional modes has been growing in recent years, with their intermediate OAM values enabling finer control in the applications mentioned above [2].

The structure of fractional modes has been predicted by Berry to be a chain of off-axis vortices, arising from their expression as a superposition of integer modes [5]. The field of a paraxial fractional mode is

$$\psi_\ell(R, \phi, z) = \frac{\exp(i\pi\ell) \sin(\pi\ell)}{\pi} \sum_{n=-\infty}^{\infty} \frac{1}{\ell - n} \psi_n(R, \phi, z) \quad (2)$$

n is an integer and ℓ is a fraction.

The arrangement of these integer vortices in a fractional vortex beam has also been shown experimentally in terms of both intensity and phase [6, 7]. However, also predicted by Berry is the absence of vortices on the z-axis [5] — that is, the phase no longer has azimuthal dependence at $R = 0$:

$$\psi_\ell(R = 0, z) = \frac{\exp(i(z + \pi\ell)) \sin(\pi\ell)}{\pi\ell} \quad (3)$$

In this work, we experimentally generate fractional vortex beams, and investigate their resulting intensity and mode. We measure the Gaussian component of these beams by projecting them on a Gaussian mode provided by a single mode fiber. In contrast to the mentioned experiments, whose focus is on the arrangement and stability of these vortices, we aim to describe these vortex beams instead by the absence of vortices on the z-axis. This is equivalent to examining their Gaussian ($\ell = 0$) component, which can be done through a Gaussian single mode fiber.

2 Methods

Figure 1 shows the schematic diagram of the experimental setup used to generate and characterize fractional vortex beams. A beam from a He-Ne laser ($\lambda = 633$ nm) is expanded using a set of lenses and illuminated the surface of a spatial light modulator (SLM – Pluto Holoeye). We uploaded holograms H onto the SLM of the fractional vortex beams of the form,

$$H \propto |E_{obj} + E_{ref}|^2 \quad (4)$$

where E_{obj} is the electric field of the fractional vortex given in equation (1), and E_{ref} is the electric field of the reference beam. Upon reflecting off from the SLM, we isolated the first diffractive order using a pinhole. The intensity profiles of these fractional modes were captured using a CCD camera (Point Grey FlyCap).

Next, to measure the strength of the Gaussian mode, we use a single mode fiber (SMF) connected to a photodetector that measures the intensity as voltage. This photodetector is connected to the oscilloscope for us to record the optical signal. We removed the beam splitter in the experimental setup to allow the full intensity into the SMF. The beam size is further reduced by a pair of lenses for it to fully fit into the fiber. The exiting beam — the projection — is registered in the photodetector and the corresponding voltages were measured by the oscilloscope at 2500 samples/second. We vary the value of ℓ — from $0.0 \leq \ell \leq 1.0$ with interval of 0.05, then with interval of 0.1 beyond that.

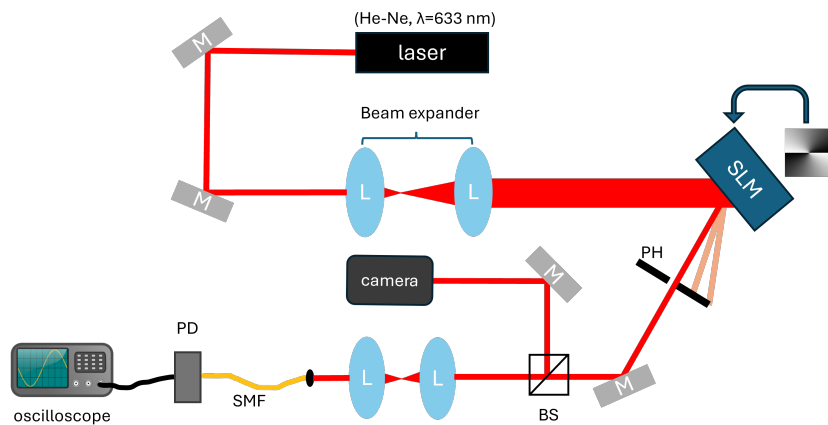


Figure 1: Schematic diagram of the experimental setup. Collimated light from the laser hits the surface of the SLM where the hologram of the fractional vortex beam is uploaded. We select the first diffraction order using a pinhole (PH) and mirror (M), measure the corresponding Gaussian component using a single mode fiber (SMF) connected to a photodetector (PD) as we change the value of ℓ .

3 Results & Discussion

One of the distinguishing features of integer vortex beams is the dark region at their center, resulting from the phase singularity. This characteristic is why these beams are also referred to as doughnut modes. Figure 2 shows the experimentally generated fractional and vortex beams with the setup shown in Figure 1. Among integer vortices, we observe that a larger ℓ corresponds to a larger dark central region, consistent with previous results [8]. However, when having non-integer or fractional topological charges, dark stripes and circular fringes arise as seen in the figure. These features exhibit the evolution of the vortex wherein it begins from a “tear” on the right side and then gets absorbed by the dark region forming larger vortices. Also noticeable on profiles of $\ell \neq 0$ are dark concentric rings. These features can be attributed to the edge-diffracted waves described by the Bessel function in (1), formed when we use fractional topological charges ℓ as calculated by [5]. From the raw voltage reading from the oscilloscope, we obtain mean voltage reading per fractional charge ℓ to get the Gaussian component of the fractional vortex as shown in Figure 3. As expected, the curve peaks at $\ell = 0$ where the incident beam coincides with the mode of the single mode fiber. We also observe that for integer values of $\ell \neq 0$, the voltage is close to zero which can be explained by orthogonality principles between the incident light and the mode of the SMF.

However, a different phenomenon occurs when the topological charge is fractional, especially when ℓ is near half-integer values. Looking at just the images, it is not immediately intuitive that the Gaussian component would peak at half-integers for $\ell > 1$. But, as seen in the voltage curve, we observe peaks

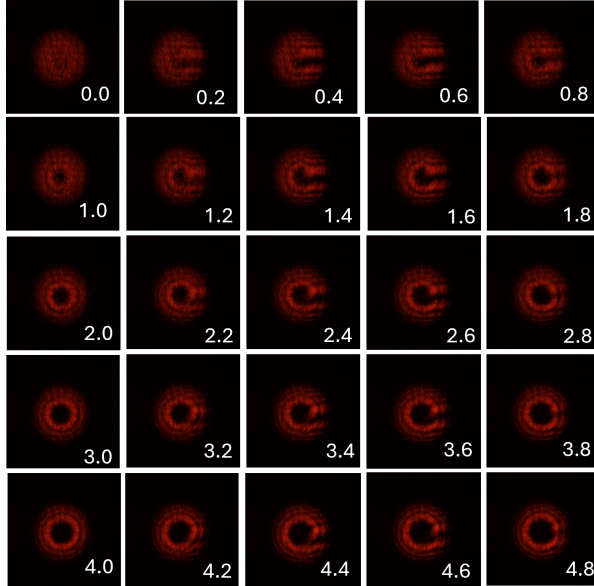


Figure 2: Intensity profiles of vortex beams at different $0.0 \leq \ell < 5.0$. Non-integer vortex modes have a characteristic ‘‘tear’’ on their right side, unlike the uniform distribution of Gaussian mode ($\ell = 0$) and doughnut modes (integer ℓ).

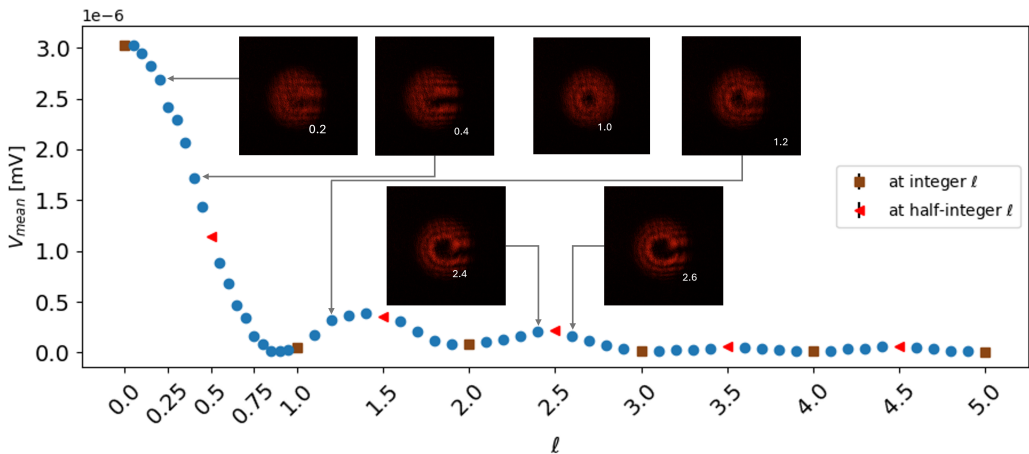


Figure 3: Mean voltage V_{mean} representing the Gaussian component at each value of ℓ . The voltage curve has local peaks for half integer values of ℓ (e.g. $\ell = 1.5, 2.5$). Errorbars (black) are obscured by the markers.

near half-integer values (e.g., $\ell = 1.5, 2.5$, etc.). We believe these peaks arise due to the occurrence of $\ell = 0$ modes. As first predicted by Berry [5] and experimentally demonstrated by Leach et al. using phase measurement techniques [6], for half-integer ℓ values, a line of alternating charge vortices forms near the radial discontinuity. These alternating charge vortices result from the birth of a vortex that occurs when ℓ passes a half-integer step. Since the nearest integer to the fractional vortex ℓ increases by unity when ℓ passes a half-integer step, an extra vortex must be created [5]. Additionally, we observe an overall decrease in the peaks as ℓ increases, which may be explained by the increasing radius of the central dark region, as seen in the images of the integer modes in Figure 2.

Initially, the smaller interval of data collection within $\ell \in [0, 1]$ was to evaluate the alignment of the beam with the fiber — that is, the voltage should decrease in that range, of ℓ as $\ell = 1$ is the first orthogonal mode. However, the monotony of the decreasing voltage in this range of ℓ more explicitly demonstrates the same ‘‘tearing’’ of the beam from the outer right, since there is no pre-existing central dark region.

4 Conclusions

In this study we have projected fractional vortex beams onto a Gaussian mode carried by a single mode fiber to study their Gaussian component. We analyzed our results, guided both by the predictions of Berry — as well as the intensity profiles which were consistent with these predictions. In particular, we focused on the Gaussian components at (and near) integer and half-integer ℓ , showing consistency with Berry's predictions as well. Our results have thus demonstrated the study of the Gaussian component — or the absence of vortices — as an alternate description of fractional vortex beams, without looking at the precise positions of the vortices in the beams themselves.

Although we have attributed the qualities of our images and Gaussian component to the predictions of Berry, we recommend to calculate the specific power of the mode projection between the fractional vortex and the Gaussian mode to get a more precise description of the Gaussian component of the beam. This can be done by evaluating the overlap integral $\int \psi_\ell^* \psi_0 \, dA$ over cross-sectional area dA where ψ_0 is the Gaussian mode of the single mode fiber. To verify the existence of other modes in fractional vortex beams, one can also implement a modal decomposition similar to [9]. Additionally, our methods may be extended, as an alternate characterization, to previous studies [7] of the fractional vortices at different propagation distances.

Acknowledgments

The authors would like to thank DOST Philippine Council for Industry, Energy and Emerging Technology Research and Development (PCIEERD Project No. 04002), and the University of the Philippines Office of the Vice President for Academic Affairs thru its Balik-PhD Program (OVPAA-BPhD 2015-06) for financial support. NZ Simon would like to acknowledge the Office of the Chancellor of the University of the Philippines Diliman, through the Office of the Vice Chancellor for Research and Development, for funding support through the Thesis and Dissertation Grant (Project No. 232310 DNSE).

References

- [1] Y. Yang, Y. Ren, M. Chen, Y. Arita, and C. Rosales-Guzmán, Optical trapping with structured light: a review, *Adv. Photonics* **3**, 034001 (2021).
- [2] H. Zhang, J. Zeng, X. Lu, Z. Wang, C. Zhao, and Y. Cai, Review on fractional vortex beam, *Nanophotonics* **11**, 241 (2022).
- [3] S. N. Alperin, R. D. Niederriter, J. T. Gopinath, and M. E. Siemens, Quantitative measurement of the orbital angular momentum of light with a single, stationary lens, *Opt. Lett.* **41**, 5019 (2016).
- [4] F. Cardano and L. Marrucci, Twisted photons: what is the orbital angular momentum of light?, *Photoniques* **119**, 62 (2023).
- [5] M. V. Berry, Optical vortices evolving from helicoidal integer and fractional phase steps, *J. Opt. A: Pure Appl. Opt.* **6**, 259 (2004).
- [6] J. Leach, E. Yao, and M. J. Padgett, Observation of the vortex structure of a non-integer vortex beam, *NJP* **6**, 71 (2004).
- [7] S. Matta, P. Vayalamkuzhi, and N. K. Viswanathan, Study of fractional optical vortex beam in the near-field, *Opt. Commun.* **475**, 126268 (2020).
- [8] M. J. Padgett, F. M. Miatto, M. P. Lavery, A. Zeilinger, and R. W. Boyd, Divergence of an orbital-angular-momentum-carrying beam upon propagation, *NJP* **17**, 023011 (2015).
- [9] M. Vasnetsov, V. Pas'ko, and M. Soskin, Analysis of orbital angular momentum of a misaligned optical beam, *NJP* **7**, 46 (2005).

Appendix

This Github repository (<https://github.com/mimmpphi/phase-holes-SPP-MIMM>) contains the MATLAB program (SLM control), Python program (data processing), and raw data.